E213 : Analysis of Decays of heavy vector boson Z^0

A lab report written by

Group P20: Mrunmoy Jena and Ajay Shanmuga Sakthivasan

Supervisor: Martin Angelsmark

Universität Bonn

May 20, 2022

Contents

Introduction

Theoretical Background

1.1 The Standard Model- A Brief Overview

The Standard Model of particle physics which has been one of the most successful and well-tested theories so far, provides the most fundamental description of nature by incorporating the elementary particles and their interactions. These elementary particles are categorized into two families: fermions (having half integer spins) which form matter as we know it, and bosons (with integer spins) serving as mediators of the three fundamental forces. While electromagnetic interactions are mediated by the photon (γ); strong and weak interactions are mediated by gluons (g) and by $W^{\pm}, Z^0$ bosons respectively. A fundamental particle that mediates gravitation has been only postulated theoretically, and is left out of the Standard Model, since the effects of gravity are too weak to play any important role in the realm of particle physics. The fermions consists of three generations of quarks and leptons. The quarks have six flavours: up (u), down (d), charm (c), strange (s), top (t) and bottom (b). Similarly, the leptons consist of the electron (e), muon (μ) and tau (τ), each having its own associated charge-less and almost massless neutrino (ν_e, ν_μ and ν_τ). Furthermore, each particle in the standard model has its own antiparticle. The quarks are able to form composite particles in either three quark combinations, called baryons ($qqq/\bar{q}\bar{q}\bar{q}$) or a quark-antiquark pair, called a meson ($q\bar{q}$). Mathematically, the elementary particles are described as elements of representations of certain symmetry groups. The gauge fields that couple to these particles (i.e. mediate the interactions) arise naturally as a consequence of invariance of their corresponding Lagrangian under local group transformations [1]. As such, the gauge symmetry that governs the Standard Model is given by:

$$SU(3)_{\text{Colour}} \times SU(2)_{\text{Left chiral}} \times U(1)_{\text{Y(Weak hypercharge)}}$$

1.2 The Unified Theory of Electromagnetic and Weak Interactions

Since the experiment deals with verifying some of the properties of the Z^0 bosons, it is of interest to touch upon the theory of electroweak unification.

While electromagnetism and the theory of weak interactions were formulated separately, it was later on postulated that at higher energies ($\sim$ 246 GeV [2]), both these interactions would be unified into a single force. As such, the GSW(Glashow-Salam-Weinberg) electroweak model was developed in the 1960s to describe this unified force.

One finds that imposing the principle of local gauge invariance on the $SU(2)_L$ symmetry group leads to the introduction of three gauge fields: $W^{(1)}$, $W^{(2)}$ and $W^{(3)}$ (or W^0 in some references) [1]. The physical W^+ and W^- bosons (that mediate the weak charged current interaction) can be seen as the linear combinations:

$$W^{\pm} = \frac{1}{\sqrt{2}}\left(W^{(1)} \mp W^{(2)}\right) \tag{1.1}$$

However, the $W^{(3)}$ field has no physical interpretation of its own. Therefore an additional symmetry, the $U(1)_Y$ group is introduced. The field B (or equivalently Y^0) arising as a consequence of this new symmetry, similarly does not have a physical meaning on its own. Rather, it was seen that linear combinations of the $W^{(3)}$ (W^0) and B (Y^0) fields gives rise to the photon and the Z^0 boson:

$$\begin{pmatrix} \gamma \\ Z^0 \end{pmatrix} = \begin{pmatrix} \cos\theta_W & \sin\theta_W \\ -\sin\theta_W & \cos\theta_W \end{pmatrix} \begin{pmatrix} B \\ W^{(3)} \end{pmatrix} \tag{1.2}$$

where θ_W is the weak mixing/Weinberg angle

In addition to this, it is to be noted that the gauge fields $W^{(1),(2),(3)}$ and B have to be massless, in order to respect gauge invariance under local $SU(2)_L \times U(1)_Y$ gauge transformation. However, the physical gauge bosons $W^{\pm}$ and Z^0 are predicted to be massive, whereas the photon should remain massless. To explain this, the concept of electroweak spontaneous symmetry breaking was introduced. A massive scalar field (the Higgs field) is introduced, to which these bosons ($W^{\pm}$, Z^0) must couple to, in order to get their physical masses, while the photon does not interact with it [3]. The intricacies of the Higgs mechanism are not of immediate interest here, and can be understood from standard references [1, 4].

1.3 Physics Related to the Z^0 Resonance

1.3.1 e^+e^- Interactions

Before discussing the processes of interest involving Z^0 production, we first list out the important ways in which e^+e^- pairs can interact [5]:

- $\boldsymbol{e^+e^- \to e^+e^-}$: Bhaba scattering (elastic scattering) of e^+e^- pairs
- $\boldsymbol{e^+e^- \to e^+e^-\gamma\gamma}$: two photon process; e^+e^- can scatter off of virtual photons, arising out of the incoming e^- and e^+ themselves and these photons can then produce hadrons
- $\boldsymbol{e^+e^- \to f\bar{f}}$: Electron-positron pairs annihilate to produce a gauge boson (γ or Z^0), which would in turn produce a fermion-antifermion ($f\bar{f}$) pair. Here $f\bar{f}$ are fermions other than e^+e^- since that process is already included under Bhaba scattering.
- $\boldsymbol{e^+e^- \to \gamma\gamma/\gamma\gamma\gamma}$: An electron-positron pair could also produce two or three photons

In case of the lowest order $e^+e^- \to f\bar{f}$ process, there are contributions to cross section from pure Z^0, pure γ as well as from $\gamma - Z^0$ interference terms. However, near center of mass energies close to the Z^0 resonance, the major contribution to the total cross section is from the pure Z^0 term.

Additionally, it is easy to see that for the particular case of $e^+e^- \to e^+e^-$ scattering (Bhaba scattering), there is a t-channel contribution in addition to the s-channel component.

1.3.2 Forward-Backward Asymmetry

1.3.3 Background Processes: Radiative Corrections

1.3.4 Important Parameters of a Resonance Particle

1.4 Physics of High Energy Colliders

Pre-Lab Exercises

In this chapter, we have provided our solutions to some theoretical questions that were needed to be solved before conducting the experiment. All the equations and standard values of parameters used to calculate the numerical results for these exercises are taken from [5], unless mentioned otherwise.

2.1 Calculation of partial decay widths for $Z^0 \to f\bar{f}$

In this exercise, we are required to calculate the partial decay widths of $Z^0 \to f\bar{f}$; where $f\bar{f}$ represent the following fermion-antifermion pairs : (i) e^+e^- (ii) $\mu^+\mu^-$ (iii) $\tau^+\tau^-$ (iv) $q\bar{q}$, where q represents all the flavours of quarks (except for t quark, because it is too heavy ($M_t \approx 172.76$ GeV [6]) to be produced from Z^0 decays). The partial decay widths have been calculated with the following formula:

$$\Gamma_f = \frac{N_c^f \sqrt{2}}{12\pi} G_F M_Z^3 \left(\left(g_V^f\right)^2 + \left(g_A^f\right)^2 \right) \tag{2.1}$$

where:

N_c^f: colour factor, (1 for leptons, 3 for quarks)

$G_F = 1.16637 \times 10^{-5}\text{GeV}^{-2}$, Fermi's constant

$M_Z = 91.182$ GeV, mass of Z^0 boson

$g_V^f = I_3^f - 2Q_f \sin^2\theta_W$, vector coupling strength of Z^0 to fermions

$g_A^f = I_3^f$, axial-vector coupling strength of Z^0 to fermions

Q_f: electric charge of fermion f

I_3: third component of weak isospin

$\sin^2\theta_W = 0.2312$, θ_W is the Weinberg (weak-mixing) angle

Fermion	$\mathbf{Q_f}$	$\mathbf{I_3^f}$	$\mathbf{g_V^f}$	$\mathbf{g_A^f}$	$\mathbf{N_c^f}$	$\mathbf{\Gamma_f^{(calc)}}$ **/MeV**	$\mathbf{\Gamma_f^{(ref)}}$ **/MeV**
e^-, μ^-, τ^-	-1	-0.5	-0.0376	-0.5	1	83.89	83.8
u, c	2/3	0.5	0.1917	0.5	3	285.34	299
d, b, s	-1/3	-0.5	-0.3459	-0.5	3	367.84	378
ν_e, ν_μ, ν_τ	0	0.5	0.5	0.5	1	165.85	167.6

Table 2.1: Parameters $Q_f, I_3^f, g_V^f, g_A^f, N_c^f$ for various fermion pairs and their partial decay widths

The calculated partial decay widths for the required fermion pairs have been listed under $\Gamma_f^{(calc)}$ in Table 2.1. Further, the reference [5] values of partial decay widths for the same fermion pairs are listed under $\Gamma_f^{(ref)}$ for comparison. We have also included the partial decay widths of the three neutrinos since they would be used in the solution to the next exercise.

One finds that calculated values of partial decay width for the lepton pairs are in close agreement with the literature value, deviating by about 0.1% to 1%. The slight deviation could be caused because the

$\gamma \to f\bar{f}$ term and interference terms have been neglected. In case of the quarks, the deviations from the reference values are higher ($\sim$ 2.7% to 4.6%). This may be due to the fact that additionally, the effect of strong interactions have not been accounted for in our calculations.

2.2 Calculation of hadronic, leptonic and total decay widths and cross section

Hadronic decay width: The decay widths for the hadronic mode is given by the sum of the partial decay widths of the u,d,c,s and b quarks:

$$\Gamma_{had} = \Gamma_u + \Gamma_c + \Gamma_d + \Gamma_s + \Gamma_b = 2 \cdot \Gamma_{u,c} + 3 \cdot \Gamma_{d,s,b} = 1674.20 \text{ MeV}$$

'Charged' decay width: The charged leptons, e, μ, τ will contribute to this decay width:

$$\Gamma_{charged\ leptonic} = \Gamma_e + \Gamma_\mu + \Gamma_\tau = 3 \cdot \Gamma_{e,\mu,\tau} = 250.17 \text{ MeV}$$

'Neutral' (invisible) decay width: The uncharged leptons ($\nu_e,\ \nu_\mu,\ \nu_\tau$) will contribute to this:

$$\Gamma_{neutral\ leptonic} = \Gamma_{\nu_e} + \Gamma_{\nu_\mu} + \Gamma_{\nu_\tau} = 3 \cdot \Gamma_{\nu_e} = 497.55 \text{ MeV}$$

Total Z^0 decay width: The total decay width for Z^0 will just be the sum of the hadronic, charged leptonic and neutral leptonic decay widths:

$$\Gamma_{total} = \Gamma_{hadronic} + \Gamma_{charged\ leptonic} + \Gamma_{neutral\ leptonic} = 2421.92 \text{ MeV}$$

Partial cross sections at maximum of resonance: At resonance, the formula for calculating partial cross section for $Z^0 \to f\bar{f}$ becomes:

$$\sigma_f^{peak} = \frac{12\pi\Gamma_e\Gamma_f}{M_Z^2\Gamma_Z^2} \tag{2.2}$$

The calculated partial cross sections for the different decay channels along with the respective decay widths are tabulated in Table 2.2.

Decay channel	**Decay width / MeV**	**Partial cross section / 10^{-11} MeV^{-2}**
Hadronic (u,d,c,s,b)	1674.20	10.79
Charged leptonic (e, μ,τ)	250.17	1.61
Neutral leptonic ($\nu_e,\ \nu_\mu,\nu_\tau$)	497.55	3.21
Total	2491.92	15.61

Table 2.2: Calculated decay widths and partial cross sections for different Z^0 decay channels

2.3 Effect of additional generation on width of Z^0 resonance curve

In case it is possible for the Z^0 to decay into an extra generation of light fermions (u,d,e,ν), the total decay width will increase, and the new total decay width will be:

$$\Gamma_{total}^{(new)} = \Gamma_{total} + \Gamma_e + \Gamma_\nu + \Gamma_u + \Gamma_d = 3324.34 \text{ MeV}$$

The percentage increase in the width of the Z^0 resonance curve will be:

$$\frac{\Gamma_{total}^{(new)} - \Gamma_{total}}{\Gamma_{total}} = \frac{902.42}{2421.92} \times 100\% = 37.26\%$$

2.4 Angular distributions of differential cross sections

On studying the dependence of differential cross sections of e^+e^- processes on the azimuthal angle θ, it is found that the s-channel has a symmetrical dependence on θ (with an additional small asymmetric term, in the case of Z^0 mediated process; which will be calculated later):

$$\left(\frac{d\sigma}{d\Omega}\right)_s \propto \left(1 + \cos^2\theta\right) \tag{2.3}$$

For the case of a t-channel process, it is found that the differential cross section diverges quickly at small θ values [5]:

$$\left(\frac{d\sigma}{d\Omega}\right)_t \propto (1 - \cos\theta)^{-2} \tag{2.4}$$

While the process $e^+e^- \to \mu^-\mu^+$ can only take place through the s-channel; the $e^+e^- \to e^+e^-$ process can occur through both s and t channels. The angular distributions of these two processes are shown in Figure 2.1. For the $e^+e^- \to e^+e^-$ process, the contributions from the s and t channels are shown separately as well as their combined contribution to the differential cross section.

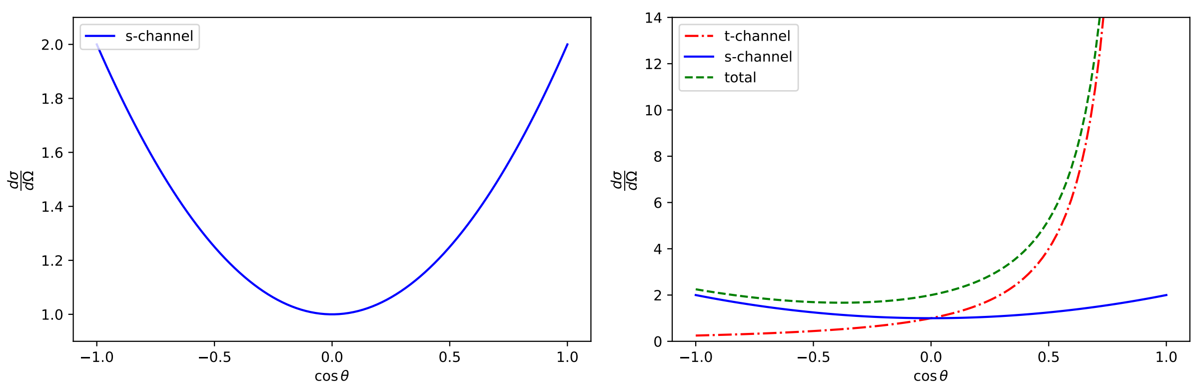

Figure 2.1: Angular distributions of $e^+e^- \to \mu^+\mu^-$ (left) and $e^+e^- \to \mu^+\mu^-$ (right)

2.5 Calculation of forward-backward asymmetry

We are required to calculate the forward-backward asymmetry factor, A_{FB} in the process $e^+e^- \rightarrow \mu^+\mu^-$. In order to do this, the following formula is used:

$$A_{FB} = \frac{3F_2}{4F_1} \tag{2.5}$$

where the parameters are given by:

$$F_1(s) = Q_f^2 - 2v_e v_f Q_f \mathfrak{Re}(\chi) + (v_e^2 + a_e^2)(v_f^2 + a_f^2)|\chi|^2$$

$$F_1(s) = -2a_e a_f Q_f \mathfrak{Re}(\chi) + 4v_e a_e v_f a_f |\chi|^2$$

$$v_f = \frac{g_V^f}{2\sin\theta_W \cos\theta_W}$$

$$a_f = \frac{g_A}{2\sin\theta_W \cos\theta_W}$$

$$\chi(s) = \frac{s}{\left((s - M_Z^2) + is\frac{\Gamma_Z}{M_Z}\right)}, \text{ Propagator}$$

s: Square of centre-of-mass energy

$\sqrt{s}$ / GeV → $\sin^2\theta_W$ ↓	89.225	91.225	93.225
0.21	-0.0937	0.0762	0.2317
0.23	-0.1639	0.0228	0.1965
0.25	-0.1948	0.0042	0.1906

Table 2.3: Forward backward asymmetry factors for different Weinberg angles (θ_W) and centre of mass energies ($\sqrt{s}$)

Analysis

3.1 Analysis of Event Displays

3.2 Part II: Statistical Analysis of Z^0 Decays

In the previous subsection, we carried out an analysis based on event displays. This was possible because we did not have a lot of events to work with. Obviously, such an analysis would prove to be futile if we try to carry it out on a large set of data. Analysis of large sets of data would be the primary discussion of this subsection. We use the software, *ROOT* to analyse the data on a statistical basis. *ROOT* works with *.root* files, which contain all the information in a tree-like structure, called *ntuple*. The contents of the *ntuple* are,

- RUN: Run number
- EVENT: Event number
- NCHARGED: Number of charged tracks
- PCHARGED: Total scalar sum of track momenta
- E_ECAL: Total energy in electromagnetic calorimeter
- E_HCAL: Total energy in hadronic calorimeter
- E_LEP: LEP beam energy ($= \sqrt{s}/2$)
- COS_THRU: cos(polar angle) between beam axis and thrust axis
- COS_THET: cos(polar angle) between incoming positron and outgoing positive particle

We also have two categories of data, each containing a lot of *ntuples*,

- Monte Carlo (MC): These correspond to the "*pure*" events from the previous subsection. These are simulated - detector response to a calculated outgoing momentum four-vector for a specific process.
- Data: These correspond to the "*mixed*" events from the previous subsection. These are real life data recorded with the OPAL detector at specific energies around the Z^0 resonance maximum.

ROOT can be used to set cuts on the above variables in a data and get histograms of different variables. This allows for a statistical analysis of the data. All the above information can be found in [5].

3.2.1 Refining the cuts

As mentioned previously, we have two categories of data. There are four Monte Carlo (MC) data, one for each of the decay channels. There are six real world data and we will be using *data6.root* for our analysis in the following parts. Analysis of event displays already gave us an idea of what cuts to use, to extract the different channels. Our first step here will be to test our cuts on the MC data and check

how they fare. And the second step will be to refine the cuts a little so that we are better able to extract different channels.
When it comes to e^-e^+ final state decay channel, we would like to exclude t-channel events. This is because t-channel is possible only in the mode and for the sake of consistency, we would like to limit ourselves to only s-channel. From theory[5], we know that the t-channel dominates at large $cos\theta$. By introducing a new cut to exclude events with large $cos\theta$, we eliminate a most of the t-channel events. But this also means that we are eliminating some of the s-channel events. To account for this, we multiply the observed events after applying the modified cuts with correction factor. This correction factor is given by,

$$\delta = \frac{\int_{-1}^{1}(1+x^2)dx}{\int_{-0.9}^{0.5}(1+x^2)dx} \approx 1.5829. \tag{3.1}$$

This factor is arrived at from theory, which gives the behaviour of s-channel as proportional to $(1+cos^2\theta)$ and the integral limits are correspond to the $cos\theta$ values which we exclude.
When it comes to $\mu^-\mu^+$ final state decay channel, we observed a lot of events with $PCHARGED$ equal to exactly 0. These events are not physical. Hence we apply a cut to eliminate such events. In the cases of e^-e^+ and $\mu^-\mu^+$, we also exclude $cos\theta$ values very close to 1 and -1, as the detector resolution is far from perfect close to the beam axis. To summarise, we have the following additions - $cos\theta \in [-0.9, 0.5]$, to remove t-channel events in the case of e^-e^+, $PCHARGED > 0$, to exclude unphysical events in the case of e^-e^+ and $cos\theta \in [-0.9, 0.9]$, to eliminate low resolution events in the cases of e^-e^+ and $\mu^-\mu^+$. Interestingly, the channels $\tau^-\tau^+$ and $q\bar{q}$ did not require any additional global cuts. But, we did add the cut $cos\theta \in [-1, 1]$ to remove any unphysical events.
After testing our cuts, we arrive at the conclusion that we don't need any further refinements other than the additions mentioned above. With these additions, we go about analysing *data6.root*. The raw data of observed events using our cuts is given in the table 3.1 below. Note that the correction factor has not been applied to the e^-e^+ event numbers but it is used in our latter calculations. The event numbers are exactly what we get after applying all the cuts appropriately.

	Number of observed events				
MC Sample	e^-e^+ cuts	$\mu^-\mu^+$ cuts	$\tau^-\tau^+$ cuts	$q\bar{q}$ cuts	Total (incl. global cuts, if any)
e^-e^+	18835	0	378	0	56720
$\mu^-\mu^+$	0	76209	8599	0	89887
$\tau^-\tau^+$	26	35	71131	135	79214
$q\bar{q}$	0	0	173	92164	98563

Table 3.1: Number of events with different cuts applied to each of the MC data.

3.2.2 Efficiency Matrix

The efficiency matrix is a measure of how efficient the cuts are at extracting the different decay channels. If we consider the actual event numbers of the different channels as a 4×1 matrix, the efficiency matrix will be a 4×4 matrix and ideally, it should be a unit matrix. In this case, the event numbers observed matches the actual event numbers. But this is not the case usually. We should aim to achieve an efficiency matrix with diagonal elements as close to 1 as possible and the off-diagonal elements as close to 0 as possible. The efficiency matrix elements are given by[5],

$$\epsilon_{ij} = \frac{N_j^{i,cut}}{N_j^{j,all}}. \tag{3.2}$$

For example, ϵ_{12} corresponds to e^-e^+ cuts applied to $\mu^-\mu^+$ events divided by the total observed $\mu^-\mu^+$ events. Note that we construct the 4×1 matrix in the following order - e^-e^+ events, $\mu^-\mu^+$ events, $\tau^-\tau+$ events and $q\bar{q}$ events. With this efficiency matrix, one could extract the actual event numbers as follows,

$$N_{obs} = \epsilon N_{actual} \implies N_{actual} = \epsilon^{-1} N_{obs}. \tag{3.3}$$

This gives us an efficiency matrix,

$$\epsilon = \begin{pmatrix} 5.26 \times 10^{-1} & 0 & 3.28 \times 10^{-4} & 0 \\ 0 & 8.48 \times 10^{-1} & 4.42 \times 10^{-4} & 0 \\ 6.66 \times 10^{-3} & 9.57 \times 10^{-2} & 8.98 \times 10^{-1} & 1.76 \times 10^{-3} \\ 0 & 0 & 1.70 \times 10^{-3} & 9.35 \times 10^{-1} \end{pmatrix}. \tag{3.4}$$

Given a cut, whether or not a particular event passes it can be modelled with a binomial distribution, just like modelling a coin toss. In the limit when such an "experiment" is conducted on large sample size, the probability mass function of the binomial distribution can be approximated by a normal distribution. In which case, the standard deviation is given by,

$$\Delta\epsilon_{ij} = \sqrt{\frac{\epsilon_{ij}(1-\epsilon_{ij})}{N}}, \tag{3.5}$$

where ϵ_{ij} is a particular element of the efficiency matrix and N is the total events corresponding to that matrix element. The above treatment can be found in any introductory book on probability theory, for example Feller[7]. This gives us the standard deviation in the efficiency matrix elements,

$$\Delta\epsilon = \begin{pmatrix} 2.10 \times 10^{-3} & 0 & 6.44 \times 10^{-5} & 0 \\ 0 & 1.12 \times 10^{-3} & 7.47 \times 10^{-5} & 0 \\ 3.41 \times 10^{-4} & 9.81 \times 10^{-4} & 1.08 \times 10^{-3} & 1.33 \times 10^{-4} \\ 0 & 0 & 1.46 \times 10^{-4} & 7.85 \times 10^{-5} \end{pmatrix}. \tag{3.6}$$

For our calculations in the following sections, we require N_{actual}. Therefore, we invert the matrix. The calculations for error in the inverse matrix elements is not straightforward. We refer to [8], which gives the error in the inverse matrix element to be,

$$(\Delta\epsilon^{-1})_{ij}^2 = \sum_{\alpha=1}^{4}\sum_{\beta=1}^{4}(\epsilon^{-1})_{i\alpha}^2(\Delta\epsilon)_{\alpha\beta}^2(\epsilon^{-1})_{\beta j}^2. \tag{3.7}$$

With this we get the following inverse efficiency matrix and the error in the inverse efficiency matrix elements,

$$\epsilon^{-1} = \begin{pmatrix} 1.90 & 7.85\times10^{-5} & -6.95\times10^{-4} & 1.30\times10^{-6} \\ 7.36\times10^{-6} & 1.18 & -5.80\times10^{-4} & 1.09\times10^{-6} \\ -1.41\times10^{-2} & -1.26\times10^{-1} & 1.11 & -2.09\times10^{-3} \\ 2.57\times10^{-5} & 2.29\times10^{-4} & -2.03\times10^{-3} & 1.07 \end{pmatrix} \pm \begin{pmatrix} 7.59\times10^{-3} & 1.54\times10^{-5} & 1.36\times10^{-4} & 2.75\times10^{-7} \\ 1.30\times10^{-6} & 1.67\times10^{-3} & 9.81\times10^{-5} & 2.02\times10^{-7} \\ 7.26\times10^{-4} & 1.31\times10^{-3} & 1.33\times10^{-3} & 1.59\times10^{-4} \\ 2.58\times10^{-6} & 1.98\times10^{-5} & 1.75\times10^{-4} & 8.98\times10^{-4} \end{pmatrix} \tag{3.8}$$

3.2.3 Cross Sections

With the above inverse efficiency matrix, we can now calculate the actual event numbers and hence, the cross sections corresponding to different modes. The actual event numbers, N_{actual}, will simply be $\epsilon^{-1}N_{obs}$, as explained earlier. The error in actual event numbers is then,

$$\Delta N_{obs,i} = \sqrt{\sum_{j=1}^{4} N_{obs,j}^2(\Delta\epsilon_{ij}^{-1})^2 + \sum_{j=1}^{4}(\epsilon_{ij}^{-1})^2 N_{obs,j}}. \tag{3.9}$$

The events are assumed to obey Poisson statistics and hence, ΔN_{obs} is taken as $\sqrt{N_obs}$. With the actual event numbers, we can calculate the cross section as,

$$\sigma = \frac{N_{actual}}{\int \mathcal{L}dt} + \text{cf(radiation)}, \tag{3.10}$$

with the errors,

$$\Delta\sigma = \sqrt{\frac{(\Delta N_{actual})^2}{(\int \mathcal{L}dt)^2} + \frac{N_{actual}^2(\Delta \int \mathcal{L}dt)^2}{(\int \mathcal{L}dt)^4}}. \tag{3.11}$$

where $\int \mathcal{L}dt$ is the integrated luminosity and cf(radiation is the radiative correction factors. We use the integrated luminosity values and the radiative correction factors from from [5]. The actual event numbers, integrated luminosity values and the radiative correction factor can be found in the tables A.1, A.2 in the appendix and the calculated cross sections for different $\sqrt{s}$ values can be found in the table 3.2.

$\sqrt{s}$ [GeV]	σ_{ee} [nb]	σ_{mm} [nb]	σ_{tt} [nb]	σ_{qq} [nb]
88.47	0.39 ± 0.03	0.30 ± 0.02	0.47 ± 0.03	7.19 ± 0.10
89.46	0.82 ± 0.04	0.65 ± 0.03	0.72 ± 0.03	14.20 ± 0.14
90.22	1.26 ± 0.04	1.16 ± 0.03	1.12 ± 0.03	25.70 ± 0.21
91.22	1.69 ± 0.02	1.82 ± 0.02	1.75 ± 0.02	40.75 ± 0.22
91.97	1.12 ± 0.05	1.32 ± 0.04	1.21 ± 0.04	28.96 ± 0.27
92.96	0.45 ± 0.04	0.55 ± 0.03	0.66 ± 0.04	13.67 ± 0.20
93.71	0.28 ± 0.03	0.34 ± 0.02	0.40 ± 0.03	8.20 ± 0.13

Table 3.2: Calculated cross section values for different $\sqrt{s}$ values.

3.2.4 Forward Backward Asymmetry and Weak mixing angle

The Z^0 boson couples differently to left- and right-handed fermions. This leads to an asymmetry in the angular distribution of final state particles. This asymmetry depends, not very surprisingly, on the weak mixing (or Weinberg) angle[1]. Therefore, by calculating this asymmetry between the forward and backward scattering particle, we can measure the weak mixing angle. We consider the $\mu^-\mu^+$ decay channel as we don't have the problem of t-channel like in the e^-e^+ decay mode. We also get two clear tracks in the case of $\mu^-\mu^+$ decay mode. We can calculate the asymmetry by measure the event numbers for $cos\theta > 0$ and $cos\theta < 0$. The forward backward asymmetry then is,

$$A_{fb} = \frac{N_+ - N_-}{N_+ + N_-} + \mathrm{cf}(A_{fb}), \tag{3.12}$$

where N_+ is the event numbers with $cos\theta > 0$ and N_- is the event numbers with $cos\theta < 0$, $\mathrm{cf}(A_{fb})$ is the A_{fb} correction factor, which can be found in the table A.2. The error in A_{fb} is given by,

$$\Delta A_{fb} = \sqrt{N_- \left(\frac{2N_+}{(N_+ + N_-)^2}\right)^2 + N_+ \left(\frac{2N_-}{(N_+ + N_-)^2}\right)^2}. \tag{3.13}$$

The calculated A_{fb} can be found in table 3.3. With this, we can calculate the weak mixing angle. For

$\sqrt{s}$ [GeV]	N_+	N_-	A_{fb}
	$\mu^-\mu^+$ data		
88.47	51	69	-0.128 ± 0.090
89.46	148	156	-0.007 ± 0.057
90.22	272	319	-0.063 ± 0.041
91.22	4297	4384	0.008 ± 0.011
91.97	387	380	0.039 ± 0.036
92.96	173	123	0.231 ± 0.057
93.71	189	150	0.209 ± 0.054
	$\mu^-\mu^+$ MC		
91.22	37807	38402	0.010 ± 0.014

Table 3.3: Forward and Backward event numbers for $\mu^-\mu^+$ mode data and MC events with the calculated A_{fb} values.

the data events, we consider the A_{fb} value at Z^0 resonance energy and calculate the weak mixing angle as,

$$sin^2\theta_W = 0.2369 \pm 0.1537, \tag{3.14}$$

and for the MC event, we calculate the weak mixing angle as,

$$sin^2\theta_W = 0.2352 \pm 0.1560. \tag{3.15}$$

3.2.5 Lepton Universality

Lepton universality states that, since the masses of leptons are much smaller compared to that of the Z^0 boson, the cross section of all the three leptonic decay modes must be the same, at Z^0 resonance. From the table **??**, we can see that at Z^0 resonance ($= 91.22GeV$),

$$\begin{aligned} \sigma_e &= 1.69 \pm 0.02\text{nb} \\ \sigma_\mu &= 1.82 \pm 0.02\text{nb} \\ \sigma_\tau &= 1.75 \pm 0.02\text{nb} \end{aligned} \tag{3.16}$$

We see that even though the values are almost equal, they are not exactly equal. And in fact, they are a little far from the theoretical value as well, which is discussed later. We postulate that this is due to the fact that the efficiency matrix is not "ideal" in our case. That is, we are undercounting the event numbers to some extent, which results in the lower cross section values. And since the factor by which we undercount differs between different modes, we get cross sections that slightly differ from each other. We calculate the ratios of the hadronic to the leptonic modes as follow,

$$\begin{aligned} \frac{\sigma_{had}}{\sigma_e} &= 24.18 \pm 0.30 \\ \frac{\sigma_{had}}{\sigma_\mu} &= 22.43 \pm 0.24 \\ \frac{\sigma_{had}}{\sigma_\tau} &= 23.28 \pm 0.26 \end{aligned} \tag{3.17}$$

The ratios above directly reflect the deviations we had in the cross section values and a little greater than the theoretical value. But, both the cross section values and the ratios are of the same order of magnitude and in fact comparable to the theoretical values. This means that the problem in our data is not fundamental and could be overcome by improving our efficiency.

3.2.6 Breit-Wigner Fit of Cross Section

Now we extract the all important quantities from our data. To do this, we fit our cross section values against a Breit-Wigner curve of the form,

$$\sigma_f(s) = \frac{12\pi}{M_Z^2} \frac{s\Gamma_e\Gamma_f}{(s - M_Z^2)^2 + \left(\frac{s\Gamma_Z}{M_Z}\right)^2} (\hbar^2 c^2), \tag{3.18}$$

which has three parameters, M_Z, Γ_Z and $\Gamma_e\Gamma_f$. The factor $\hbar^2 c^2 = 3.893793719 \times 10^5$nb GeV^2 is used to convert the cross section values to SI units from natural units. We used *scipy.optimize* module for *Python* to fit the function against our data. The plots are given in 3.1. The fit parameters obtained along with the reduced χ^2 values for the fit can be found in the table 3.4. We have three parameters and

Channel	M_Z [GeV]	Γ_Z [GeV]	$\Gamma_e\Gamma_f$ [GeV^2]	χ^2_{red}
e^-e^+	90.973 ± 0.047	2.591 ± 0.158	$6.615\times10^{-3} \pm 6.29\times10^{-4}$	0.93
$\mu^-\mu^+$	91.117 ± 0.021	2.462 ± 0.060	$6.306\times10^{-3} \pm 2.46\times10^{-4}$	0.52
$\tau^-\tau^+$	91.159 ± 0.058	2.825 ± 0.179	$7.690\times10^{-3} \pm 7.85\times10^{-4}$	1.44
$q\bar{q}$	91.187 ± 0.004	2.515 ± 0.010	0.1460 ± 0.0009	0.38

Table 3.4: Fit parameters and reduced χ^2 values for the data

seven data points. This gives us 4 degrees of freedom for our fit. The e^-e^+ fit gives the best reduced χ^2 value. The reduced χ^2 values for $\mu^-\mu^+$ and $\tau^-\tau^+$ are less than 1, which implies that we are over-fitting the data or the error variances are overestimated. The reduced χ^2 value for $\tau^-\tau^+$ is greater than 1,

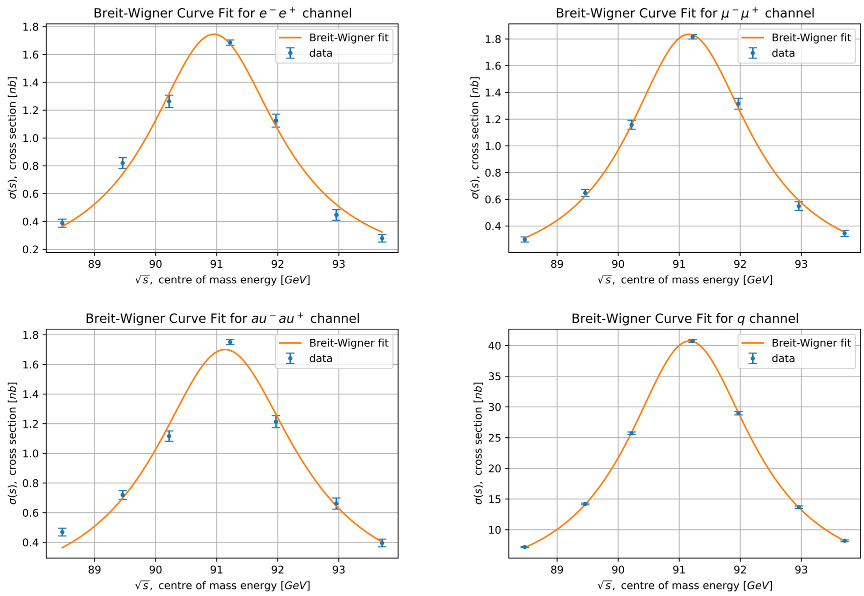

Figure 3.1: Breit-Wigner fit for the four different decay channels

which implies that we are under-fitting the data or the error variances are underestimated. But still, the reduced χ^2 values are not much larger than 1, which means they're a good fit[9].
The fit parameters directly give us the values of mass of the Z^0 boson, M_Z and the decay width of the Z^0 boson, Γ_Z. The mean value of the quantities are,

$$\begin{aligned} M_Z &= 91.123 \pm 0.020 \\ \Gamma_Z &= 2.598 \pm 0.062. \end{aligned} \tag{3.19}$$

3.2.7 Partial Width of Different Channels and Number of Light Neutrino Generations

The third fit parameter doesn't directly give us the partial decay width of different channels. It gives the product of the partial decay width of e^- mode and the partial decay width of f mode, the final state fermion in consideration. In the case of e^-e^+ channel, this reduces to Γ_e^2, which lets us calculate the partial decay width of the e^- mode. This can then been used to calculate the partial width of other channels. This is given in the table 3.5. The literature values for Γ_f are taken from [10]. The literature

Channel	Γ_f [MeV]	Γ_f (lit.) [MeV]
e^-e^+	81.33 ± 5.47	83.91 ± 0.12
$\mu^-\mu^+$	77.53 ± 6.03	83.99 ± 0.18
$\tau^-\tau^+$	94.56 ± 11.55	84.08 ± 0.22
$q\bar{q}$	1795.52 ± 121.31	1744.4 ± 2.0

Table 3.5: Partial decay width of different channels and literature values

values lie within one standard deviation of the calculated partial width, which is impressive.
With all the decay widths in hand, we can now determine the number of generations of light neutrinos. We use the value for Γ_ν from [5], which is $\Gamma_\nu = 167.6MeV$. With this, we can calculate the number of

neutrino generations using,

$$n_\nu = \frac{\Gamma_Z - \Gamma_e - \Gamma_\mu - \Gamma_\tau - \Gamma_q}{\Gamma_\nu}. \tag{3.20}$$

This gives the number of neutrino generations as,

$$n_\nu = 3.28 \pm 0.45. \tag{3.21}$$

This tells us that number of neutrino generations are 3. And within one standard deviation, our result absolutely excludes the possibility of fourth neutrino generation.

3.2.8 Discussion

Bibliography

[1] M. Thomson, *Modern particle physics* (Cambridge University Press, 2013).
[2] J. Erler and A. Freitas, *Electroweak Model and Constraints on New Physics*, English, Mar. 2018.
[3] S. K. Dooling, "Differential Cross Section Measurement of Drell-Yan Production and associated Jets with the CMS Experiment at the LHC", OA; Universität Hamburg, Diss., 2015, Dr. (Universität Hamburg, 2015), p. 242.
[4] D. J. Griffiths, *Introduction to elementary particles; 2nd rev. version*, Physics textbook (Wiley, New York, NY, 2008).
[5] Universität Bonn, *Instructions for E213: analysis of Z^0 decay.*
[6] P. Zyla et al. (Particle Data Group), "Review of Particle Physics", PTEP **2020**, and 2021 update, 083C01 (2020).
[7] W. Feller, *An introduction to probability theory and its applications, volume 1*, en, 3rd ed., Wiley Series in Probability and Statistics (John Wiley & Sons, Jan. 1968).
[8] M. Lefebvre, R. K. Keeler, R. Sobie, and J. White, "Propagation of errors for matrix inversion", `10.1016/S0168-9002(00)00323-5` (1999).
[9] P. R. Bevington and D. K. Robinson, *Data reduction and error analysis for the physical sciences* (McGraw-Hill, New York, NY, Nov. 1969).
[10] K. Olive, "Review of particle physics", Chinese Physics C **40**, 100001 (2016).

Data

Table A.1: Observed event numbers and actual events numbers for different $\sqrt{s}$ values.

$\sqrt{s}$ [GeV]	e^-e^+	$\mu^-\mu^+$	$\tau^-\tau^+$	$q\bar{q}$
			N_{obs}	
88.47	106	120	251	3281
89.46	261	304	425	7413
90.22	415	591	693	14709
91.22	4839	8581	10178	221068
91.97	393	767	863	18728
92.96	150	296	427	8100
93.71	178	339	459	8635
			N_{actual}	
88.47	202 ± 20	141 ± 13	256 ± 18	3508 ± 61
89.46	496 ± 31	358 ± 21	416 ± 23	7927 ± 92
90.22	789 ± 39	697 ± 29	661 ± 30	15729 ± 130
91.22	920 ± 137	1023 ± 111	971 ± 120	236399 ± 541
91.97	747 ± 38	904 ± 33	820 ± 33	20026 ± 147
92.96	285 ± 23	349 ± 20	419 ± 23	8662 ± 96
93.71	338 ± 25	400 ± 22	448 ± 24	9234 ± 100

Table A.2: Integrated luminosity values for *data6.root* and radiative and $\mathrm{A_{FB}}$ corrections for different $\sqrt{s}$ values.

$\sqrt{s}$ [GeV]	$\int \mathcal{L}dt[\text{nb}]^{-1}$	Rad. Correction [nb]		$\mathrm{A_{FB}}$ Correction
		Hadronic	Leptonic	
88.47	675.9 ± 5.7	+2.0	+0.09	0.021512
89.46	800.8 ± 6.6	+4.3	+0.20	0.019262
90.22	873.7 ± 7.1	+7.7	+0.36	0.016713
91.22	7893.5 ± 54.3	+10.8	+0.52	0.018293
91.97	825.3 ± 6.9	+4.7	+0.22	0.030286
92.96	624.6 ± 5.5	-0.2	-0.01	0.062196
93.71	942.2 ± 7.7	-1.6	-0.08	0.093850